Journal of Applied Polymer Science

Light-scattering properties of linear low density polyethylene/polystyrene films fabricated through layer-multiplying technology

Shanshan Luo, Juan Xue, Ying Xiong, Jiabin Shen, Shaoyun Guo
State Key Laboratory of Polymer Materials Engineering, Polymer Research Institute of Sichuan University, Chengdu, Sichuan 610065, China
Correspondence to: J. Shen (E-mail: shenjb@scu.edu.cn)

ABSTRACT: The material consisting of alternating layers of a linear low density polyethylene (LLDPE)/polystyrene (PS) blend (90/10 wt/wt) and pure poly(methylmethacrylate) (PMMA) was prepared through layer-multiplying extrusion. The LLDPE/PS light-scattering films were obtained by peeling off the PMMA layers. Morphological examination demonstrated that the PS particles were dispersed as spherical domains in all the LLDPE/PS layers and the average diameter increased from skin to core layers. When a laser beam was vertically incident on the individual layers, the one located in the skin layer had a stronger light-scattering pattern than that located in the core layer. All the LLDPE/PS films had a similar transmittance close to 90%, while the haze tended to decrease from the skin layer toward the core layer. The Mie's scattering theory was applied to analyze the influence of morphological evolution on the light scattering behaviors. © 2016 Wiley Periodicals, Inc. J. Appl. Polym. Sci. **2016**, *133*, 43826.

KEYWORDS: blends; morphology; properties and characterization

Received 16 November 2015; accepted 24 April 2016
DOI: 10.1002/app.43826

INTRODUCTION

Light diffusing films are translucent films which can scatter incident light in different directions. They have been widely used in the backlight unit of liquid crystal display (LCD) devices to assure uniform luminance.[1–3] In addition, they can also save cost and energy due to reduced consumption of light bulbs when applied in electroluminescent signs or LED luminaries.[4] With the improvement of living standards, the demand for light-scattering films has been increasing gradually.[5] Furthermore, light diffusing materials can also be applied in other fields, including sunroofs, skylights, covers for automotive lights, etc.[6]

Typically, light diffusing materials are manufactured by dispersing inorganic particles, such as $BaSO_4$, $CaCO_3$, TiO_2, and ZnO,[7,8] in a polymer matrix. The scattering ability is determined by the difference of refractive indices between particles and matrix as well as the concentration. However, effective light diffusing materials should have excellent light transmission and good scattering properties. A large difference of refractive indices and high concentration may result in negative effects on the light transmission.[9] It has been found that the combination of both organic polymer particles and inorganic particles in a thermoplastic matrix leads to an increased transmission with good light scattering.[10–12] Low concentrations of the inorganic particles with suitable organic particles can achieve good light scattering effects,[13] but there are also several problems: it is difficult to disperse these particles uniformly in the matrix; since inorganic particles are hard and irregularly shaped, they will abrade the surface of the processing equipment; and the cost of organic particles is relatively high due to their complicated synthesis processes.

The application of polymeric blends to produce light scattering materials can avoid the above-mentioned problems and it has attracted extensive interest during recent years.[1,14–17] These incompatible compositions comprise a transparent polymer as matrix, and a polymer with a different index of refraction as the dispersed phase. The light scattering ability depends largely on the morphology of the light diffusing sheet.[18] However, a skin-core structure is frequently observed in a polymer blend system after melt processing.[19–23] Fellahi *et al.*,[22] for instance, highlighted a significant skin-core structure of injection molded high density polyethylene/polyamide-6 blend in which the dispersed phase was highly oriented in the subskin and spherical in the core. A similar structure was also observed by Yang *et al.*[23] for a typical skin-core heterogeneous distribution of microfibrils was preserved in the polycarbonate matrix after the extrusion process. The relationship between microstructure and optical properties can be studied only if the microstructure of the composite is uniform. To our best knowledge, the skin-core structure cannot be separated layer by layer through

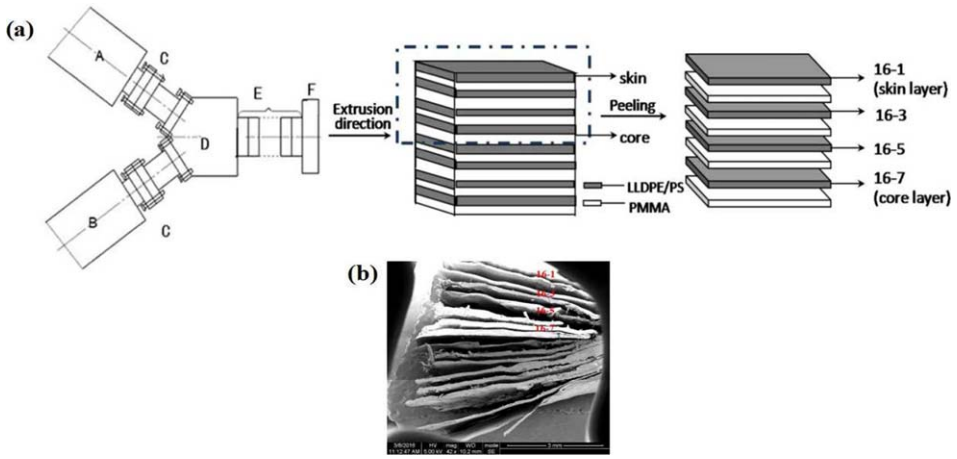

Figure 1. (a) Schematic of layer-multiplying extrusion (A, B: extruder; C: connector; D: coextrusion block; E: layer multiplying elements; F: die); (b) the SEM image of 16-layer (LLDPE/PS)/PMMA extrudate. [Colour figure can be viewed in the online issue, which is available at wileyonlinelibrary.com.] [Color figure can be viewed in the online issue, which is available at wileyonlinelibrary.com.]

conventional methods. Therefore, few reports to our knowledge have focused on studying the influence of the skin-core structure on optical properties.

Recently, an advanced force-assembly processing technology, layer-multiplying coextrusion, has been developed to prepare materials with alternating layers.[24–27] If the adjacent layers are incompatible, each layer can be peeled from the original multilayer specimen completely (Figure 1), which provides a convenient way to obtain the skin and core layers of an extrudate. Hence, an 16-layer material consisting of alternating layers of a linear low density polyethylene (LLDPE)/polystyrene (PS) blend (90/10 wt/wt) and pure poly(methylmethacrylate) (PMMA) was prepared in this work. The LLDPE/PS films located at the skin and core layers of the multilayer extrudate were obtained by peeling off the PMMA layers. The morphological development of PS from the skin to core layers and its influence on light diffusing properties for the individual layers was investigated and analyzed based on the Mie's scattering theory.

EXPERIMENTAL

Materials

LLDPE, grade 318B was provided by Saudi Basic Industry Corp. (Saudi Arabia) with a melt flow rate of 3.0 g/10 min (190 °C/2.16 kg) and a density of 0.918 g/cm^3. PS, grade 383M was provided by Chi-Mei Corp. (China) with a melt flow rate of 3.0 g/10 min (200 °C/5 kg) and a density of 1.05 g/cm^3. The refractive indices of the LLDPE and PS were measured by using an Abbe refractometer (WYA (2WAJ), Shanghai Precision and Scientific Instrument Corp., China). All specimens were prepared by compression molding at 200 °C with a mirror surface. The mirror surface faced the refracting prism of the refractometer and α-bromonaphthalene was employed as contacting liquid between the mirror surface and the refracting prism to minimize the surface reflection and to avoid the total reflection at the surface of the specimen. In this work, the measured refractive index of LLDPE and PS were 1.5100 and 1.5895, respectively. PMMA, grade CM211 was purchased from Chi-Mei Corp. (China) with a melt flow rate of 16 g/10 min (230 °C/3.8 kg) and a density of 1.19 g/cm^3.

Samples Preparation

LLDPE was blended with 10 wt % PS using a twin-screw extruder and then granulated. The temperature gradient was varied between 150 and 190 °C from hopper to die. Subsequently, PMMA and LLDPE/PS pellets were coextruded using a layer-multiplying coextrusion device. The details of this device were introduced in previous papers.[24–27] 16-layer (LLDPE/PS)/PMMA sheets consisting of 8 LLDPE/PS blend layers and 8 PMMA layers were fabricated. The temperatures of the two extruders were set as 220 °C for LLDPE/PS blend, 240 °C for the PMMA. PMMA is incompatible with the LLDPE/PS blend, thus the LLDPE/PS films can easily be feeling off from adjacent PMMA layers. And they are labeled as 16-1, 16-3, 16-5, 16-7…16-15 from the top surface to the opposite side surface as schematically shown in Figure 1(a). In this work, 16-1, 16-3, 16-5, and 16-7 were chosen to study the PS morphology development from the skin to core layers of the original multilayer extrudate. The thickness of each LLDPE/PS film was maintained around 80 μm.

Morphological Observation

The layer structure of the extrudate material and the morphologies of the LLDPE/PS layers were observed through scanning

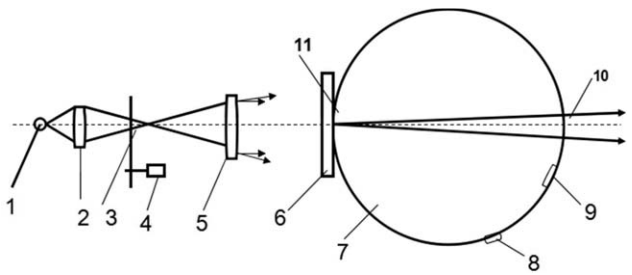

Figure 2. Optical system of the transmittance-haze instrument: (1) source; (2) condenser; (3) aperture; (4) modulator; (5) lens; (6) sample; (7) integrating sphere; (8) photocell; (9) reflectance standard; (10) emergent window; (11) entrance window.

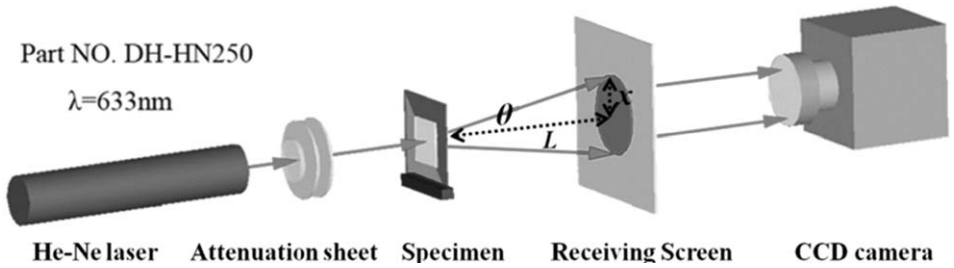

Figure 3. Schematic of light scattering testing instrument.

electron microscopy (SEM, Inspect F, FEI Co. Ltd., The Netherlands). The specimen was immersed in liquid nitrogen for 3 h and then the surface along the extrusion direction was sputtered with a thin layer of gold for observation.

Optical Measurements

Transmittance (T) and haze (H) were measured using a Transmittance-Haze testing instrument (WGT-S, Shanghai Precision and Scientific Instrument Corp., China), according to ASTM D1003-61. As schematically shown in Figure 2, all transmitted light (T) including direct (linear) transmittance and scattered (diffused) transmittance within the hemisphere scope can be trapped using the integrating sphere. Haze (H) is defined as the portion of light which is scattered by more than 2.5°after passing through a sample.[28] They can be written as:

$$T = \frac{I_t}{I_0} \tag{1}$$

$$H = \frac{(I_t)_{2.5}^{90}}{I_t} \tag{2}$$

where I_t and I_0 are the intensity of the transmitted and incident light, respectively. $(I_t)_{2.5}^{90}$ is the intensity of the transmitted light with scattering angle more than 2.5°.

As shown in Figure 3 the scattering characteristics were measured using an optical test platform consisting of a He–Ne laser (λ = 633 nm, red), attenuation sheet, specimen, receiving screen, and CCD camera. In a dark room, a laser beam with suitable light intensity was vertically incident on the specimen, with the scattered beams being projected on the receiving screen. The pattern on the receiving screen was recorded by a CCD camera. Based on the scattering pattern, the scattering angle and the distribution of the transmitted light intensity can be obtained. As shown in Figure 4, the scattering angle (θ) of the transmitted light can be theoretically calculated with the follow equation:

$$\theta = \tan^{-1}(x/L) \tag{3}$$

where x is the radius of the scattering pattern, and L indicates the distance between the specimen and the receiving screen. Furthermore, the light intensity at each pixel can be obtained through the image analysis of Origin software. The relative light intensity equals to the light intensity at each pixel divided by the largest light intensity in the scattering pattern. Then, the distribution of the relative light intensity can be achieved by plotting of the relative light intensity at every pixel versus θ.

RESULTS AND DISCUSSION

Morphological Characterization

Figure 1(b) presents the layer structure of the extrudate material, it can be seen that PMMA is indeed incompatible with the LLDPE/PS blend, thus the LLDPE/PS films can be easily peeled from each multilayer specimen. Furthermore, the typical morphological observation of the LLDPE/PS blend from the skin layer (16-1) to core layer (16-7) is shown in Figure 5. Due to the higher viscosity at the processing temperature, the PS particles were dispersed as circular domains in the LLDPE matrix.

The average diameter ($\bar{d}$) of the particles was calculated by measuring more than 200 particles for each sample. The results

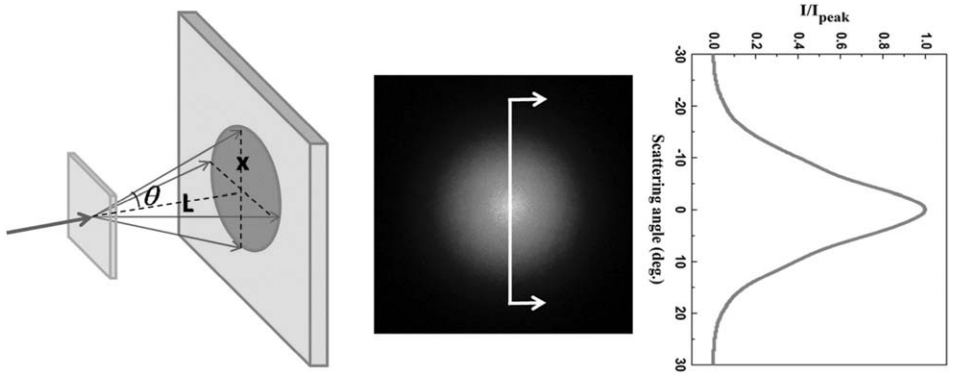

Figure 4. Schematic diagram for the relationship between relative light intensity and scattering angle.

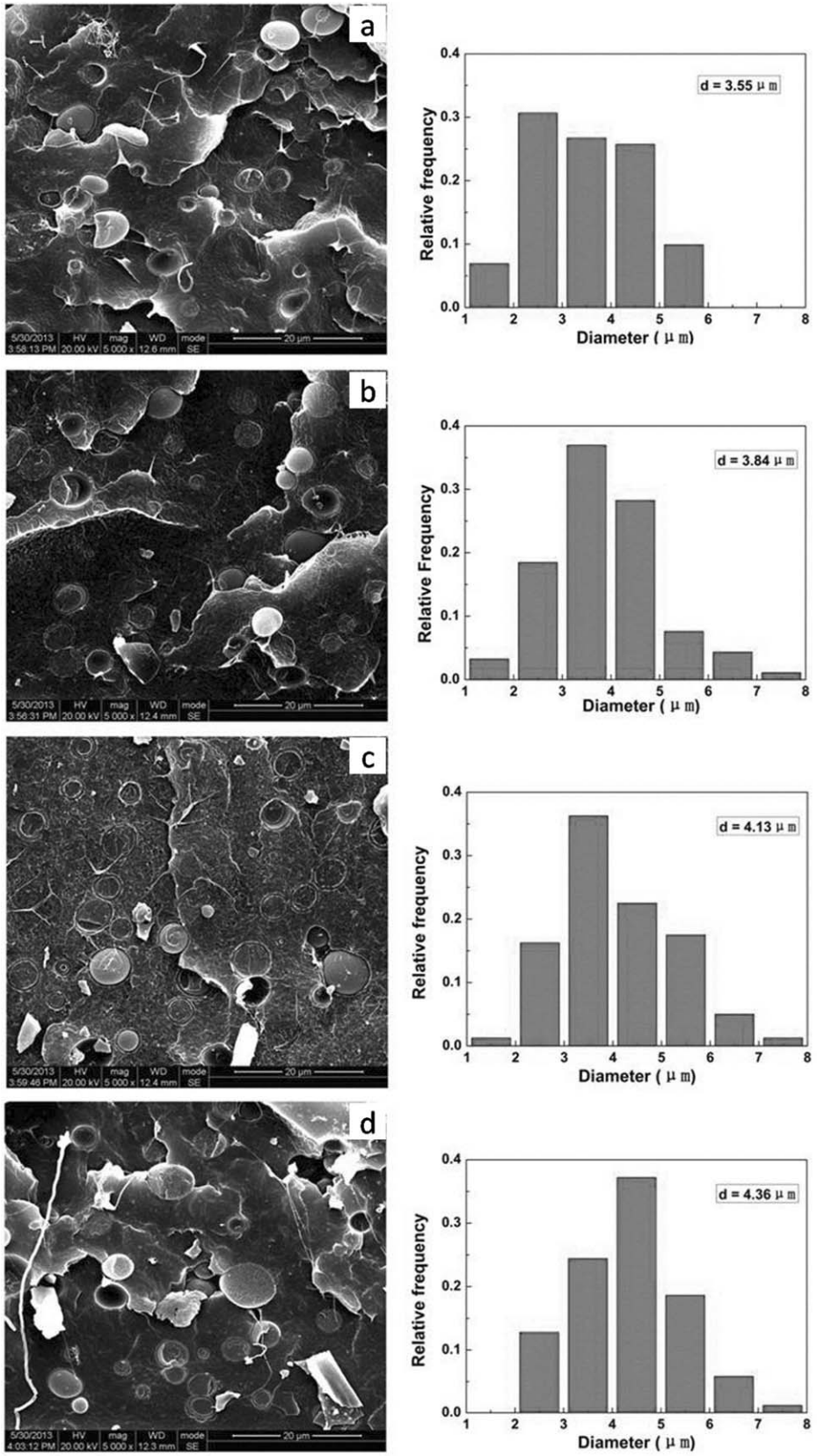

Figure 5. SEM photos of LLDPE/PS samples and statistical diameters distribution of PS phase: a. 16–1; b. 16–3; c. 16–5; d. 16–7.

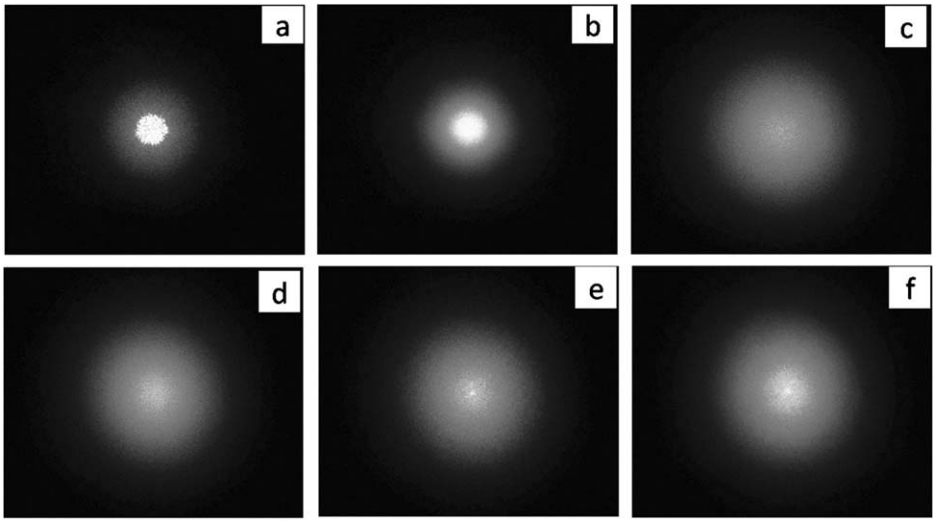

Figure 6. The photographs of scattering patterns: a. laser beam; b. pure LLDPE; c. 16-1; d. 16-3; e. 16-5; f. 16-7.

presented in Figure 5, shows that $\bar{d}$ increased from the skin layer (3.55 μm) to core layer (4.36 μm). It is known that during the extrusion process, the skin melt sustains the maximum shearing stress which may promote the breakup of the dispersed phase resulting in a smaller particle size than that in the core layer. Meanwhile, the number concentration of the particles (N) which is one of the most important parameters for determining the scattering properties was calculated through the following equation:

$$N = \frac{6\Phi}{\pi(\overline{d^3})} \tag{4}$$

where Φ is the volume fraction of the scattering phase, and d is the particle diameter. For the weight fraction of PS fixed at 10 wt %, the ratio of the number concentration is:

$$N_{16-1} : N_{16-3} : N_{16-5} : N_{16-7} = 3.78 : 2.99 : 2.40 : 2.04$$

which indicates that the number of scattering centers decreases from skin to core layers.

Optical Properties

With the laser beam vertically incident on the specimens, Figure 6 shows the scattering patterns of the LLDPE/PS blend from the skin layer (16-1) to core layer (16-7). Compared with that of the pure LLDPE sample, the optical scattering patterns of the LLDPE/PS blend films were much larger in diameter, with the light spread over a much wider angle, which means the incident laser beam was strongly scattered. Hence, we can reach the conclusion that the sphere-like PS particles dispersed in the LLDPE enhanced the light scattering. For further comparing the scattering characteristics of the LLDPE/PS blend films from skin layer (16-1) to core layer (16-7), the relative light intensities as a function of scattering angles are plotted in Figure 7. The relative light intensity is defined as the measured intensity divided by the maximum value in each scattering profile displayed in Figure 6. Hence, the scattering pattern can be quantitatively characterized by the half intensity width which is defined as the angular width when the corresponding relative light intensity is 0.5. The results show that the half intensity width of 16-1, 16-3,

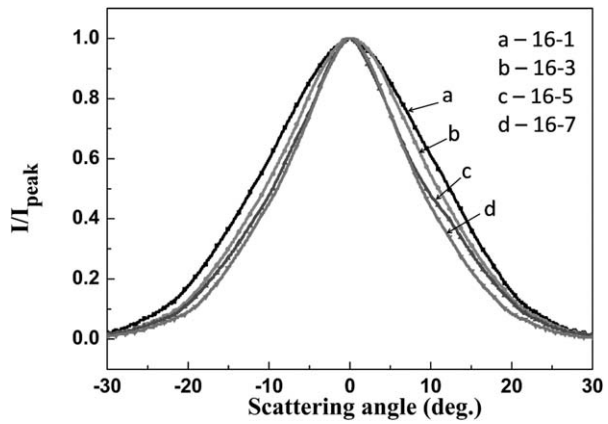

Figure 7. The relative light intensity as a function of scattering angles.

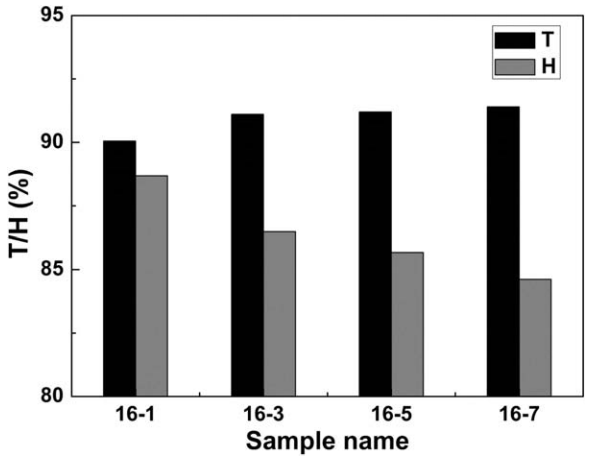

Figure 8. The transmittance and haze of the LLDPE/PS blend layers from skin to core.

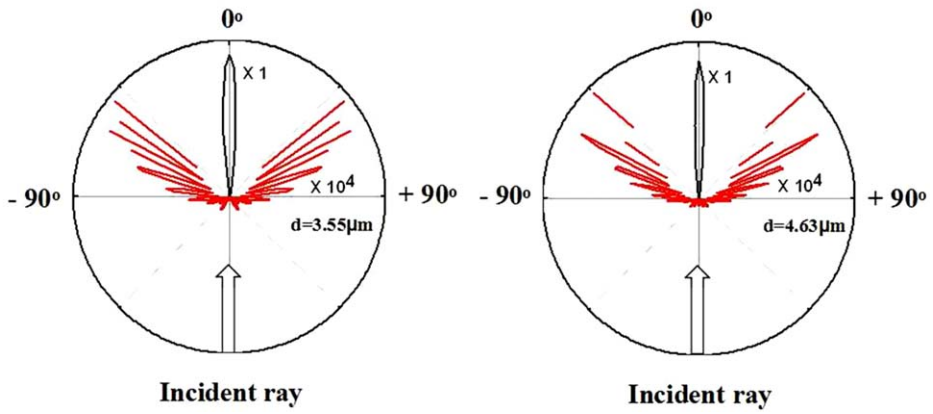

Figure 9. Calculated Mie scattering diagrams of two particles with different sizes, (a) d = 3.55 μm; (b) d = 4.63 μm. Red lines are magnified diagrams beside which magnification are marked. The refractive index: n_s = 1.5895, n_m = 1.5100. The wavelength incident light is 633 nm. [Color figure can be viewed in the online issue, which is available at wileyonlinelibrary.com.]

16-5, and 16-7 were 22.05°, 19.24°, 18.53°, and 17.75°, respectively. This result indicates that the light scattering area increased from core layer to skin layer of the LLDPE/PS blend.

Actually, a good light-scattering material must have high transmittance (T) and excellent haze (H). Figure 8 shows the T and H values of the LLDPE/PS blend layers from skin layer (16-1) to core layer (16-7). It can be noted that all four specimens had a similar T value, about 90%, while the H value tended to decrease from skin layer toward core layer and reaches the minimum in the 16-7 layer (84%). This result suggests that the particle size of PS phase plays a significant role in the H value of the LLDPE matrix.

Mie's Scattering Theory

As shown in Figure 5, the PS particles with different size were mainly dispersed as spherical domains in the LLDPE matrix, and the refractive index of PS and LLDPE were accurately measured by an Abbe refractometer. Meanwhile, for the sake of simplicity, we assume that the PS particles dispersed in LLDPE matrix have the same diameters. Hence, the light scattering characteristics of the spherical particles are theoretically analyzed using Mie's scattering theory.[29,30] According to the Mie's scattering theory, the light scattering intensity profile of a particle can be calculated as follows:

$$I(\alpha, m, \theta) = \lambda^2 (i_1 + i_2)/8\pi^2 \tag{5}$$

$$i_1 = |s_1|^2 = \left| \sum_{\upsilon=1}^{\infty} \frac{2\upsilon+1}{\upsilon(\upsilon+1)} \left\{ a_\nu \frac{P_\nu^1(\cos\theta)}{\sin\theta} + b_\nu \frac{dP_\nu^1(\cos\theta)}{d\theta} \right\} \right|^2 \tag{6}$$

$$i_2 = |s_2|^2 = \left| \sum_{\upsilon=1}^{\infty} \frac{2\upsilon+1}{\upsilon(\upsilon+1)} \left\{ b_\nu \frac{P_\nu^1(\cos\theta)}{\sin\theta} + a_\nu \frac{dP_\nu^1(\cos\theta)}{d\theta} \right\} \right|^2 \tag{7}$$

$$a_\nu = \frac{\psi'_\upsilon(m\alpha)\psi_\upsilon(\alpha) - m\psi_\upsilon(m\alpha)\psi'_\upsilon(\alpha)}{\psi'_\upsilon(m\alpha)\zeta_\upsilon(\alpha) - m\psi_\upsilon(m\alpha)\zeta'_\upsilon(\alpha)} \tag{8}$$

$$b_\nu = \frac{m\psi'_\upsilon(m\alpha)\psi_\upsilon(\alpha) - \psi_\upsilon(m\alpha)\psi'_\upsilon(\alpha)}{m\psi'_\upsilon(m\alpha)\zeta_\upsilon(\alpha) - \psi_\upsilon(m\alpha)\zeta'_\upsilon(\alpha)} \tag{9}$$

$$\alpha = 2\pi r n_m/\lambda_0 \tag{10}$$

$$m = n_s/n_m \tag{11}$$

where I is the scattering intensity, α is the size parameter, m is relative refractive index between particle (n_s) and matrix (n_m). r denotes particle radius and λ denotes wavelength in the matrix. $P_\nu^1(\cos\theta)$ is a Legendre polynomial, and ψ_υ, ζ_υ are the first two orders of the Riccati–Bessel functions. Figure 9 displays the light scattering profiles of two particles with different diameters based on eq. (5), corresponding to the number average diameters of the PS particles dispersed in 16-1 and 16-7, respectively. It can be noticed that the forward directional (−90°−90°) scattering profiles were predominant for the two particles, which corresponds to the high transmittance of the LLDPE/PS blend from skin layer to core layer as shown in Figure 8. On the other hand, the number concentration of PS particles reduces from 16-1 to 16-7 resulting in the decrease of the scattering centers, which is considered to contribute to the decrease of haze from skin layer to core layer. Furthermore, it needs to be mentioned that there were numerous PS particles dispersed in LLDPE matrix so that the multiple scattering should be considered. However, due to a wide size distribution of particles and the interference effect between adjacent particles, the accurate prediction of the multiple scattering is generally complicated.[31,32] More detailed investigation will be carried on in our future work.

CONCLUSIONS

In this work samples consisting of alternating layers of LLDPE/PS and pure PMMA were prepared through layer-multiplying coextrusion. The LLDPE/PS blends were obtained by peeling off the PMMA layers. The morphological observations showed that the PS particles were dispersed as spherical domains in the LLDPE matrix and the average diameter increased from the skin to core layer, induced by the gradient of shearing stress in the extruding process. When a laser beam was vertically incident on each LLDPE/PS film, it was strongly scattered. Compared with the film located in the core layer, the one located in the

skin layer has a larger width at half intensity denoting a wider angle of light scattering. Besides, all of LLDPE/PS films had a similar *T* value, close to 90%, while the H value tended to decrease from the skin layer to the core layer.

ACKNOWLEDGMENTS

The authors are grateful to the National Natural Science Foundation of China (51227802, 51420105004, 51421061) for financial support of this work.

REFERENCES

1. Sun, Z.; Chang, J.; Zhao, N.; Jin, W.; Wang, Y. *Optik* **2010**, *121*, 760.
2. Okumura, T.; Ishikawa, T.; Tagaya, A.; Koike, Y. *J. Opt. A: Pure Appl. Opt.* **2003**, *5*, 269.
3. Tagaya, A.; Koike, Y. *Macromol. Symp.* **2000**, *154*, 73.
4. Smith, G. B.; Earp, A.; Franklin, J. B.; McCredie, G. *Proc. SPIE* **2001**, 4458.
5. Hiraishi, M. US 6517914 B1, **2003**
6. Wu, J. C.; Work, W. J.; Dunkleberg, D.; Botnik, L.; Newman, M. US 5237004, **1993**.
7. Inagaki, K.; Yata, Y. US 4418986 A, **1983**.
8. Garica-Leiner, M. A.; Reilly, J. J.; Bradley, J.; Kryven, J. US 2012/0181489 A1, **2012**.
9. Smith, G. B.; Jonsson, J. C.; Franklin, J. *Appl. Opt.* **2003**, *42*, 3981.
10. Toshima, Y.; Kato, T. US 5852514, **1998**.
11. Eiffler, J.; Jasperse, W.; Van Heur, D.; Lee, R. *Kunststoffe* **1995**, *85*, 799.
12. Maekawa, T. US 6217176 B1, **2001**.
13. Kang, C. S.; Kim, D. J.; Kim, Y. B. US 2006/0100322 A1, **2006**.
14. Ueda, M.; Kawamura, K.; Ohno, T.; Takemura, S. EP 0464499A2, **1991**.
15. Zhou, Z.; Ma, J.; Moshrefzadeh, R. S. US 6727313 B2, **2004**.
16. Hiraishi, M.; Ohnishi, M. US 20030002153 A1, **2003**.
17. Marek, M.; Steidl, J. *J. Mater. Sci.* **2006**, *41*, 3117.
18. Tsung Lu, Y.; Chi, S. *Opt. Commun.* **2002**, *214*, 55.
19. Ghiam, F.; White, J. L. *Polym. Eng. Sci.* **1991**, *31*, 76.
20. Zhong, G. J.; Li, L. B.; Mendes, E.; Byelo, D.; Fu, Q.; Li, Z. M. *Macromolecules* **2006**, *39*, 6771.
21. Bledzki, A. K.; Faruk, O. *Compos. A: Appl. Sci. Manuf.* **2006**, *37*, 1358.
22. Fellahi, S.; Favis, B. D.; Fisa, B. *Polymer* **1996**, *37*, 2615.
23. Yang, R.; Chen, L.; Zhang, W. Q.; Chen, H. B.; Wang, Y. Z. *Polymer* **2011**, *52*, 4150.
24. Zhu, J. M.; Shen, J. B.; Guo, S. Y.; Sue, H. S. *Carbon* **2015**, *84*, 355.
25. Gao, W. L.; Zheng, Y.; Shen, J. B.; Guo, S. Y. *ACS Appl. Mater. Interface* **2015**, *7*, 1541.
26. Zheng, Y.; Dong, R. Q.; Shen, J. B.; Guo, S. Y. *ACS Appl. Mater. Interface* **2016**, *8*, 1371.
27. Chen, B. S.; Gao, W. L.; Shen, J. B.; Guo, S. Y. *Compos. Sci. Technol.* **2014**, *93*, 54.
28. ASTM 1003. Standard Test Method for Haze and Luminous Transmittance of Transparent Plastics, **1992**.
29. Mie, G. *Ann. Phys. Lpz* **1908**, *25*, 377.
30. Ungut, A.; Grehan, G.; Gouesbet, G. *Appl. Opt.* **1981**, *20*, 2911.
31. Kanemitsu, A.; Sakamoto, T.; Iyama, H. *Sumitomo Kagaku* **2007**, *2007-I*, 10.
32. Shepilov, M. P. *Opt. Mater.* **2008**, *31*, 385.